X-ray Detectors for Use with Synchrotron Radiation

Yoshiyuki Amemiya
Univ. of Tokyo, Japan

JASS'02 at Amman
October 19 – 28, 2002

Contents of the Lecture on "Detectors"

by Y. Amemiya (Univ. of Tokyo)

Photoelectric Effect → Photo electron, Auger electron, Fluorescence
or
Compton Effect → Recoiled electron

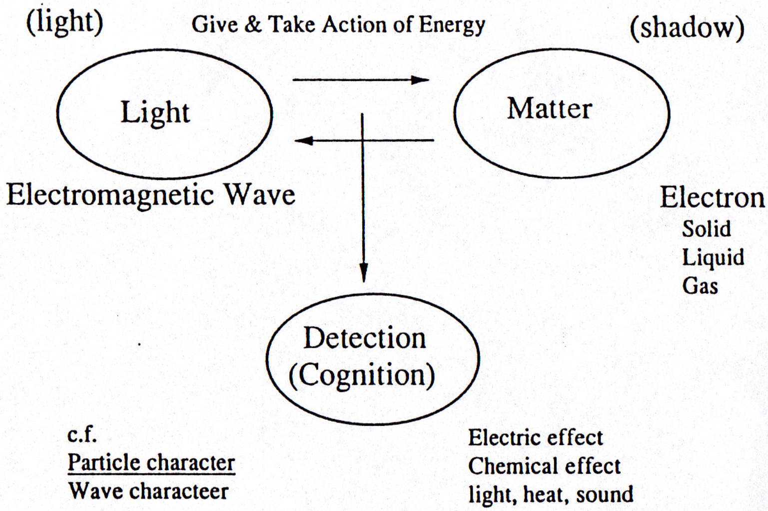

Particle character　　　　Wave character

$$E \xleftrightarrow{E=\hbar\omega} \omega$$

(Energy)　　　　(frequency)

$$E = cP \qquad\qquad \omega = ck$$

$$P \xleftrightarrow{P=\hbar k} k$$

(momentum)　　　　(wave number)

Detector

E : energy
P : position (direction)
t : time

Analyzer　$\sim 10^{18}$ Hz

phase --- coherency
polarization

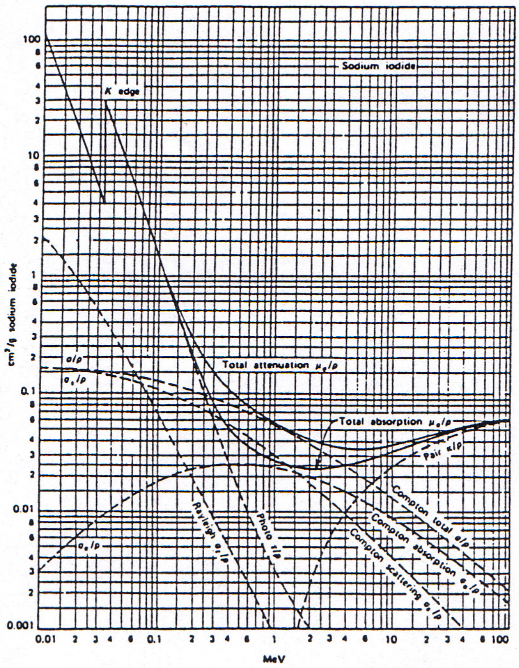

Figure 2-18 Energy dependence of the various gamma-ray interaction processes in sodium iodide. (From *The Atomic Nucleus* by R. D. Evans. Copyright 1955 by the McGraw-Hill Book Company. Used with permission.)

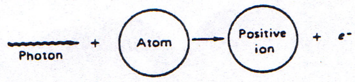

The photoelectric effect.

光電効果

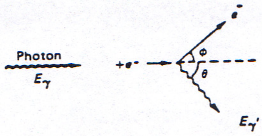

The Compton effect.

コンプトン効果

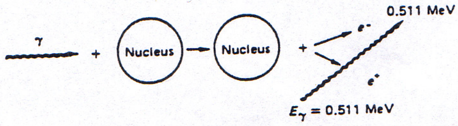

Pair production. The gamma disappears and a positron–electron pair is created. Two 0.511-MeV photons are produced when the positron annihilates.

電子対生成

Binomial Distribution

P : success probability

1 − P : otherwise (failure probability)

$$\underbrace{P(x)}_{} = \frac{n!}{(n-x)!\,x!} P^{x} (1-P)^{n-x}$$

probability of counting exactly x successes for n trials.

Assumption : success probability (P) is a constant.
$\quad\quad\quad\quad\quad\quad\quad$ ‖
each trial is independent

When

$P \ll 1$

$Pn = m = \text{constant}$

⇩

Poisson Distribution

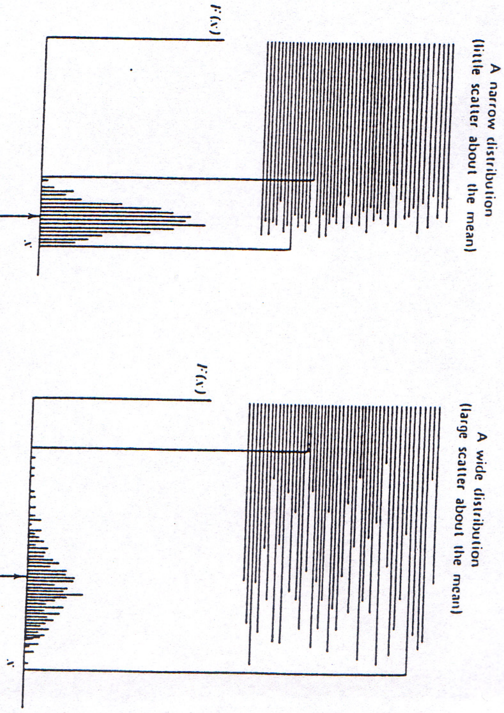

Figure 3-2 Distribution functions for two sets of data with differing amounts of internal fluctuation.

When, m (average) $\gtrsim 20$

Poisson distribution $\approx$ Normal distribution

average $= m$

variance $= m$

(S.D. $= \sqrt{m}$)

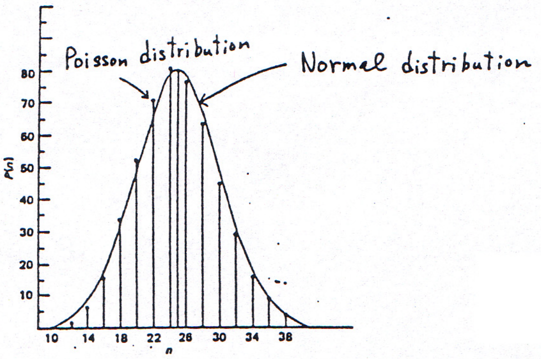

Comparison between a Poisson distribution with $m = 25$ and a Gaussian distribution with the same average and standard deviation $\sigma = \sqrt{m} = 5$.

Poisson Distribution

$$P(n) = \frac{m^n}{n!} e^{-m}$$

average $= m$

standard deviation $= \sqrt{m}$ (variance $= m$)

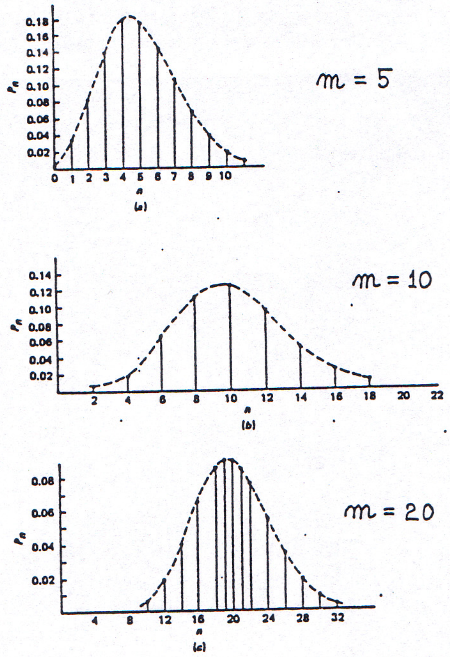

Three Poisson distributions: (a) $m = 5$, (b) $m = 10$, (c) $m = 20$.

Accuracy & Precision

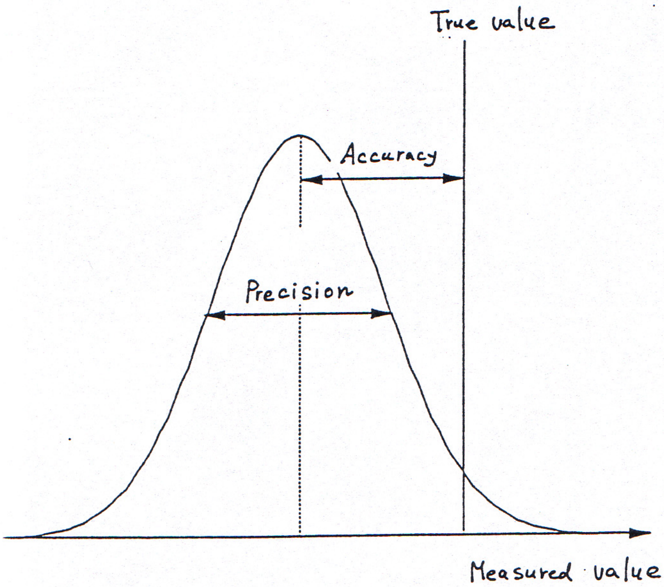

Normal distribution

The normal distribution $G(x)$ is given by

$$G(x)\,dx = \frac{1}{(\sqrt{2\pi})\sigma} \exp\left[-\frac{(x-m)^2}{2\sigma^2}\right] dx$$

where $G(x)\,dx$ = probability that the value of x lies between x and x
m = average of the distribution = 平均
σ^2 = variance of the distribution = 分散

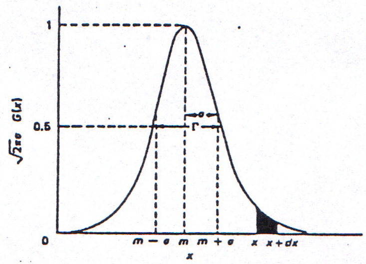

A normal (Gaussian) distribution.

$$P(m-\sigma < x < m+\sigma) = 0.68$$

$$\Gamma = \text{半値幅} \fallingdotseq 2.35\sigma$$
(FWHM)

Example 3: Multiplication or Division of Counts

$$u = xy \qquad\qquad u = \frac{x}{y}$$

$$\frac{\partial u}{\partial x} = y \;\; and \;\; \frac{\partial u}{\partial y} = x \qquad\qquad \frac{\partial u}{\partial x} = \frac{1}{y} \;\; and \;\; \frac{\partial u}{\partial y} = -\frac{x}{y^2}$$

$$\sigma_u^2 = y^2\sigma_x^2 + x^2\sigma_y^2 \qquad\qquad \sigma_u^2 = \left(\frac{1}{y}\right)^2\sigma_x^2 + \left(-\frac{x}{y^2}\right)^2\sigma_y^2$$

$$\left(\frac{\sigma_u}{u}\right)^2 = \left(\frac{\sigma_x}{x}\right)^2 + \left(\frac{\sigma_y}{y}\right)^2 \qquad\qquad \left(\frac{\sigma_u}{u}\right)^2 = \left(\frac{\sigma_x}{x}\right)^2 + \left(\frac{\sigma_y}{y}\right)^2$$

Example 4: Mean Value of Multiple Independent Counts

$$\Sigma = x_1 + x_2 + x_3 + \cdots + x_N$$

$$\sigma_\Sigma^2 = \sigma_1^2 + \sigma_2^2 + \sigma_3^2 + \cdots + \sigma_N^2$$

$$\sigma_{x_i} = \sqrt{x_i}$$

$$\sigma_\Sigma^2 = x_1 + x_2 + x_3 + \cdots + x_N = \Sigma$$

$$\sigma_\Sigma = \sqrt{\Sigma}$$

$$\bar{x} = \frac{\Sigma}{N}$$

$$\sigma_{\bar{x}} = \frac{\sigma_\Sigma}{N} = \frac{\sqrt{\Sigma}}{N} = \frac{\sqrt{N\,\bar{x}}}{N}$$

$$\sigma_{\bar{x}} = \frac{\sqrt{\bar{x}}}{N}$$

Error propagation formula

$$u = u(x_1, x_2, x_3, \cdots, x_N)$$

$$\sigma_u^2 = \left(\frac{\partial u}{\partial x_1}\right)^2\sigma_{x_1}^2 + \left(\frac{\partial u}{\partial x_2}\right)^2\sigma_{x_2}^2 + \left(\frac{\partial u}{\partial x_3}\right)^2\sigma_{x_3}^2 + \cdots$$

Example 1: Sums or Differences of Counts

$$u = x + y \text{ or } u = x - y$$

$$\frac{\partial u}{\partial x} = 1 \;\; and \;\; \frac{\partial u}{\partial y} = \pm 1$$

$$\sigma_u^2 = (1)^2\sigma_x^2 + (\pm 1)^2\sigma_y^2 \qquad\qquad \sigma_u = \sqrt{\sigma_x^2 + \sigma_y^2}$$

Example 2: Multiplication or Division by a Constant

$$u = Ax \qquad\qquad u = \frac{x}{B}$$

$$\frac{\partial u}{\partial x} = A \qquad\qquad \frac{\partial u}{\partial x} = \frac{1}{B}$$

$$\sigma_u = A\sigma_x \qquad\qquad \sigma_u = \frac{\sigma_x}{B}$$

Trinity of X-ray Instrumentation

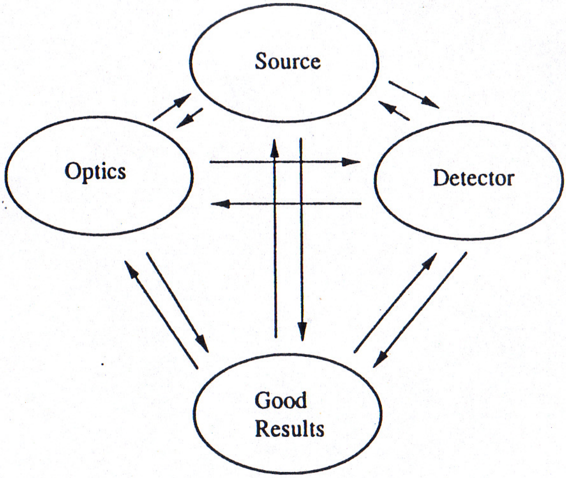

Requirements for X-ray Detectors for Use with SR
(especially for Diffraction Studies)

High counting rate (short dead time)
High sensitivity (High DQE) ------- Wide dynamic range

Linearity of response
Large active area ------------ Spatial resolution
Position accuracy (small image distortion)
Uniformity of response

Ease to handle & stability
Reasonable cost (initial & running)

Time resolution
Energy resolution
Capability for real-time measurements

Types of X-ray Detectors

	Point I	One dimensional I(x)	Two dimensional I(x,y)	Energy dimensional I(E)	Remarks
Pulse type	Scintillation counter Avalanche photo diode	1D-PSPC	2D-PSPC (MWPC)	SSD(Si, Ge) HgI2, CdTe Bolometer	High sensitivity Good linearity Wide D-range
Integration type	Ionization chamber TLD	1D-IC Photo diode array	Film Imaging plate CCD-based detector		No dead time

$$\text{dynamic range} = 20 \cdot \log \frac{\text{saturation level}}{\text{noise level}} \; [\mathrm{dB}]$$

$$= 10 \cdot \log \frac{[\text{sat. level}]^2}{[\text{noise level}]^2} \; [\mathrm{dB}]$$

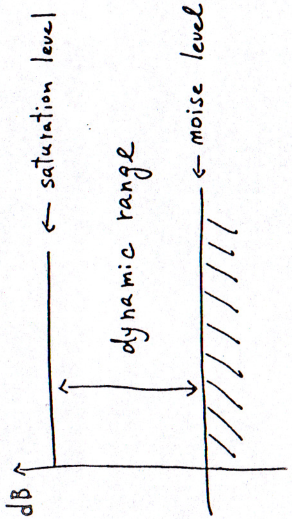

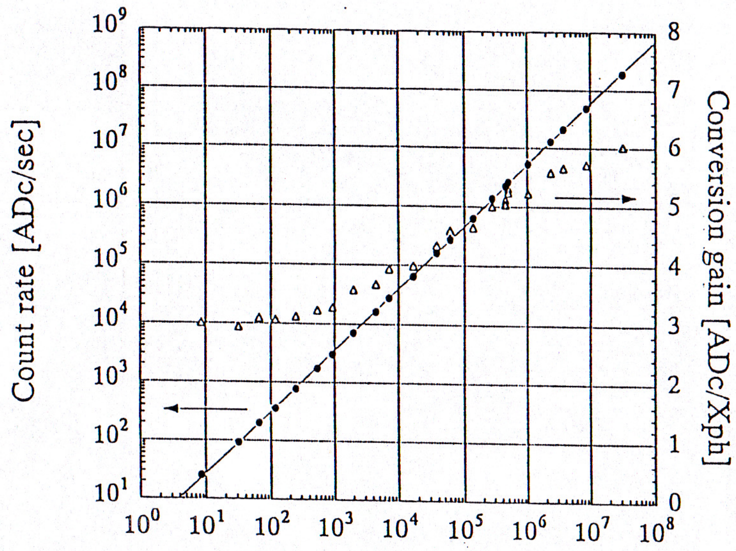

Intensity range & conversion gain of the 9-inch Be-windowed x-ray image intensifier coupled with the cooled CCD (@8 keV).

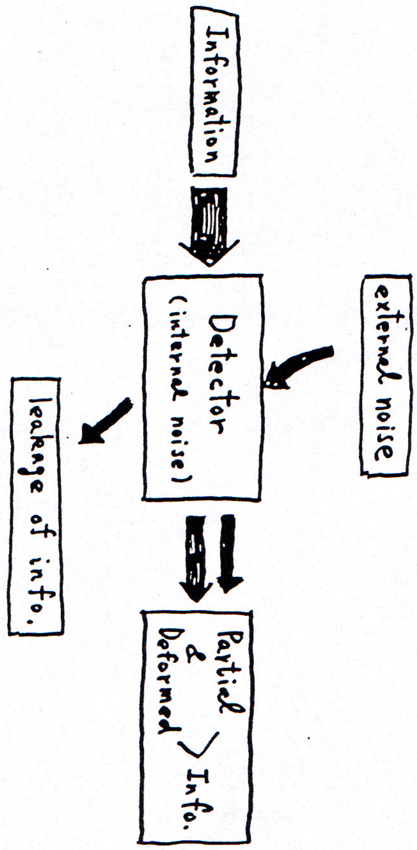

Efficiency of detectors

$\boxed{\text{Definition I}}$

$$\text{RQE} = \frac{\text{number of output events}}{\text{number of input events}}$$

Responsive Quantum Efficiency

$\boxed{\text{Definition II}}$

$$\text{DQE} = \frac{\left(\frac{S}{N}\right)^2_{\text{output}}}{\left(\frac{S}{N}\right)^2_{\text{input}}}$$

Detective Quantum Efficiency

Propagation of Errors

$\boxed{\text{Theory}}$

$$q_0 \longrightarrow \underset{\bar{n},\ \delta n}{\boxed{\ }} \xrightarrow{\ \bar{n} q_0\ } \underset{\bar{m},\ \delta m}{\boxed{\ }} \longrightarrow \bar{m}\bar{n} q_0$$

$$\text{DQE} = \frac{1}{1 + \left(\frac{\delta n}{\bar{n}}\right)^2 + \frac{1}{\bar{n}}\left(\frac{\delta m}{\bar{m}}\right)^2}$$

$\boxed{\text{ex. 1}}$

$$q_0 \longrightarrow \underset{\times 0.1}{\overset{(\text{Bi})}{\boxed{\ }}} \xrightarrow{\ 0.1\, q_0\ } \underset{\times 100}{\overset{(\text{Po})}{\boxed{\ }}} \longrightarrow 10 q_0 \pm 32\sqrt{q_0}$$

DQE = 0.099

$\boxed{\text{ex. 2}}$

$$q_0 \longrightarrow \underset{\times 100}{\overset{(\text{Po})}{\boxed{\ }}} \xrightarrow{\ 100\, q_0\ } \underset{\times 0.1}{\overset{(\text{Bi})}{\boxed{\ }}} \longrightarrow 10 q_0 \pm 10\sqrt{q_0}$$

DQE = 0.909

incident — detected (or counted)

$$q_i \longrightarrow \boxed{\text{detector}} \longrightarrow q_o$$

$$\text{DQE} = \frac{\left(\frac{S}{N}\right)^2_{out}}{\left(\frac{S}{N}\right)^2_{in}} = \frac{\left(\frac{q_o}{\sqrt{q_o}}\right)^2}{\left(\frac{q_i}{\sqrt{q_i}}\right)^2} = \frac{q_o}{q_i}$$

incident — detected — B.G. subtracted

$$q_i \longrightarrow \boxed{\text{detector}} \longrightarrow q_o + b \xrightarrow{\ -b\ } q_o$$

b

$$\text{DQE} = \frac{\left(\frac{q_o}{\sqrt{q_o + 2b}}\right)^2}{\left(\frac{q_i}{\sqrt{q_i}}\right)^2} = \frac{\frac{q_o^2}{q_o + 2b}}{q_i} = \frac{q_o}{q_i} \cdot \frac{1}{\left(1 + \frac{2b}{q_o}\right)}$$

in case of $q_o \sim b$

$$\text{DQE} \fallingdotseq \frac{q_o}{q_i} \cdot \frac{1}{1+2} = \frac{1}{3} \cdot \frac{q_o}{q_i}$$

Spatial resolution

PSF : Point Spread Function
LSF : Line Spread Function

MTF : Modulation Transfer Function

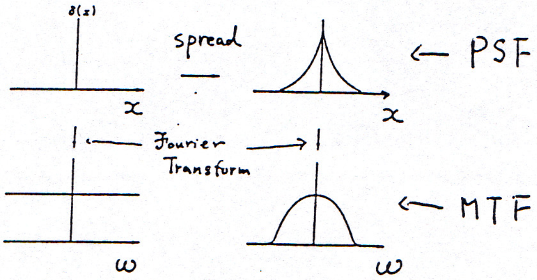

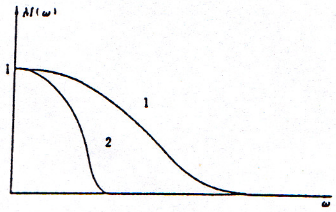

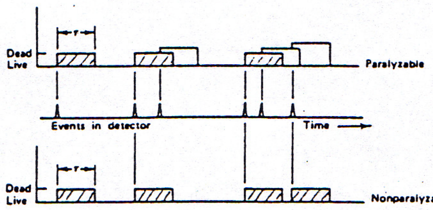

Figure 4-7 Illustration of two assumed models of dead time behavior for radiation detectors.

$$m = n e^{-n\tau}$$

$$m = \frac{n}{1 + n\tau}$$

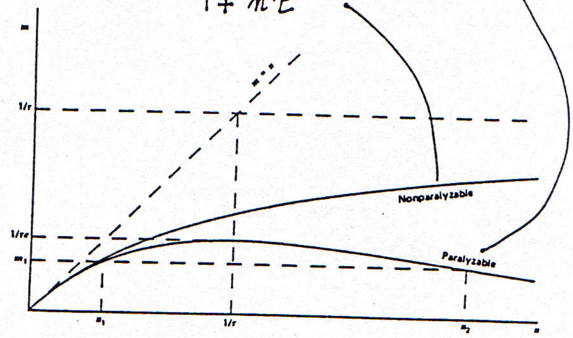

Figure 4-8 Variation of the observed rate m as a function of the true rate n for two models of dead time losses.

Energy Resolution

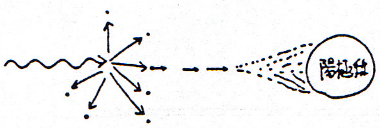

$$\underbrace{\qquad\qquad}_{n_0\text{個} \left(= \frac{E_{photon}}{W}\right)} \times A$$

$$Q = n_0 e \cdot \bar{A}$$

$$\left(\frac{\sigma(Q)}{Q}\right)^2 = \left(\frac{\sigma(n_0)}{n_0}\right)^2 + \frac{1}{n_0} \cdot \left(\frac{\sigma(A)}{A}\right)^2 \qquad (8)$$

$$\left(\frac{\sigma(n_0)}{n_0}\right)^2 = \frac{F}{n_0}$$

F : 0.05 ~ 0.2
‖
Fano Factor.

W

SSD	~ 3 eV / e^--hole
Gas Proportional Counter	~ 30 eV / e^--ion
Emulsion	~ 3 keV / grain

35 (lp/cm) at MTF 5%
↓

● MTF:

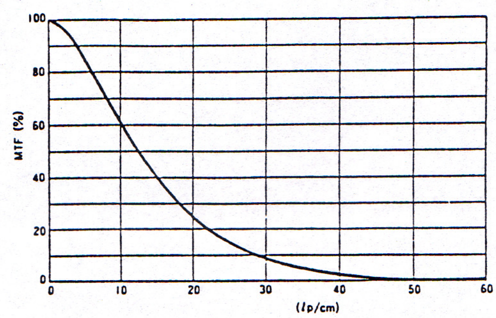

ↄ

TLD (Thermoluminescent Dosimeter)

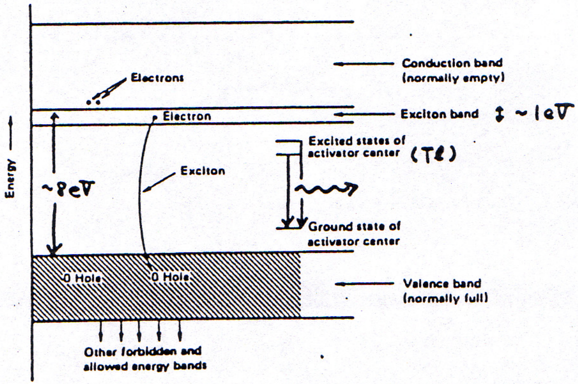

FIG. 6.2 Allowed and forbidden energy bands of a crystal.

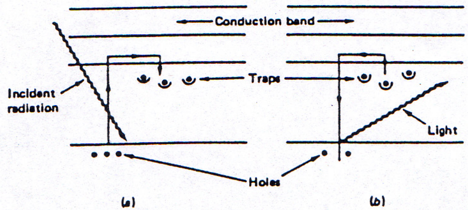

(*a*) As a result of irradiation, some carriers fall into traps. (*b*) Upon heating, the carriers are given enough energy to escape from the traps and return to the valence band, with the emission of light.

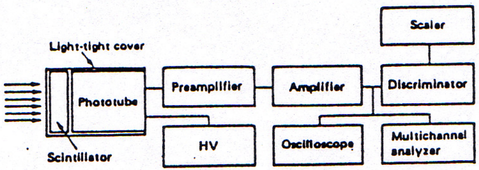

A detection system using a scintillator.

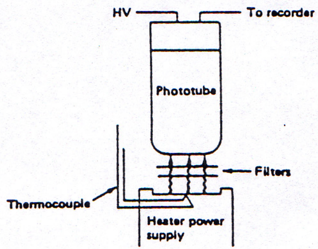

A set-up used to read a TLD.

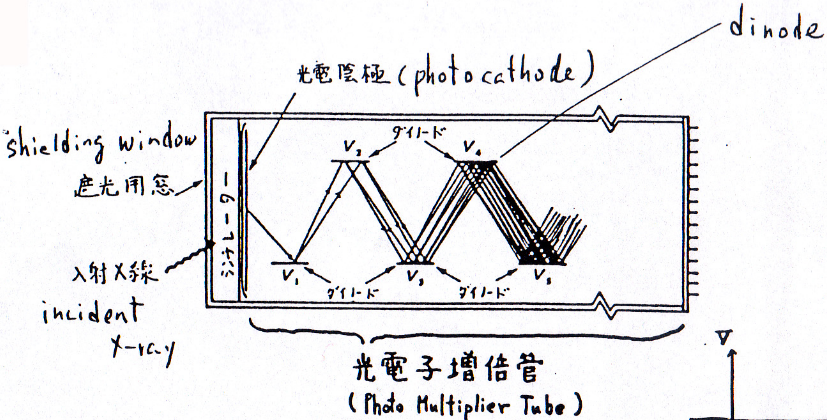

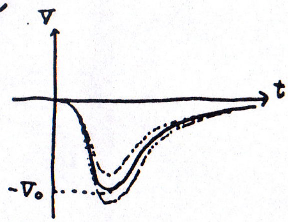

図4 シンチレーションカウンターの構造

Structure of Scintilation counter

$|V_0| \propto$ X線のエネルギー

X-ray Energy

[nA] $\quad$ photon

$i \sim 4 \times 10^{-8}\, n$ [~~粒子~~/s]

$\lambda\,[\text{Å}] = \dfrac{12.4}{E\,[\text{keV}]}$

$e = 1.6 \times 10^{-19}$ [C]

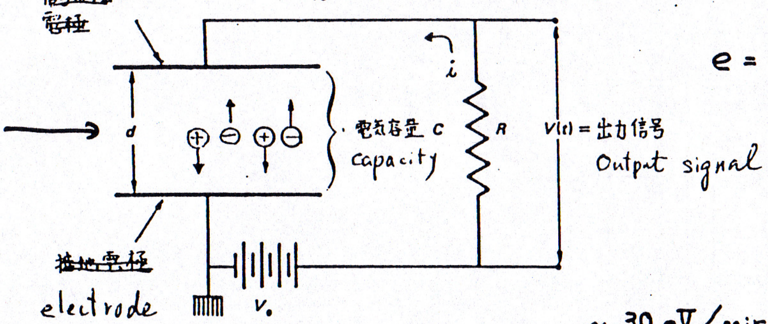

~ 30 eV/pair

for 9 keV X-ray ($\lambda = 1.4$ Å)

$\dfrac{9000\,[\text{eV}]}{\sim 30\,[\text{eV}]} = 300$ e-ion pair

Structure of Ionization chamber

図2 ~~電離箱の動作原理~~

~~エレクトロメーター(R)により電流から電圧に変換される。~~

Electric current is converted to voltage.

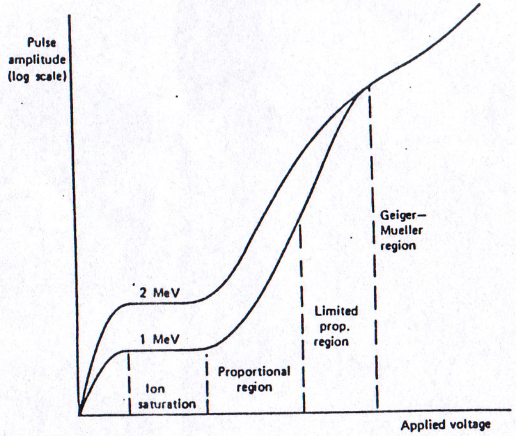

Figure 6-2 The different regions of operation of gas-filled detectors. The observed pulse amplitude is plotted for events depositing two different amounts of energy within the gas.

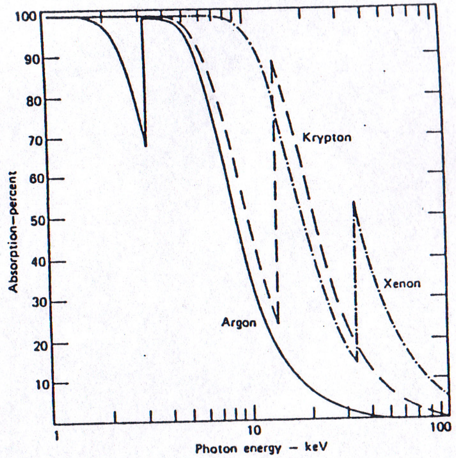

Figure 6-14 Fraction of incident photons absorbed in a 5.08 cm thick layer of several proportional gases at 1 atm pressure.

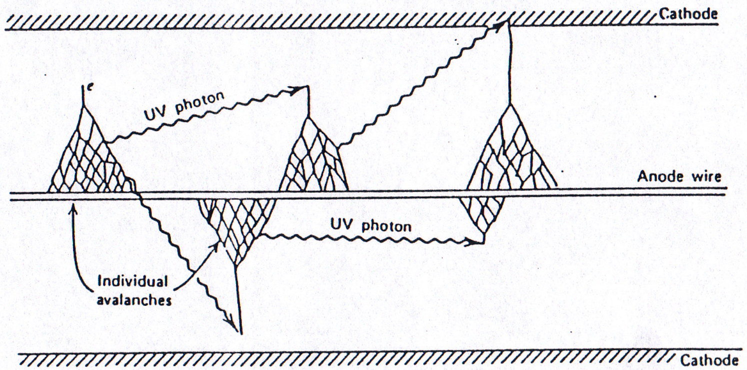

Figure 7-1 The mechanism by which additional avalanches are triggered in a Geiger discharge.

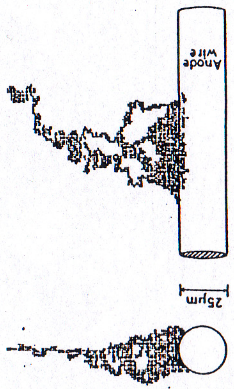

Figure 6-4 Orthogonal views of an avalanche triggered by a single electron as simulated by a Monte Carlo calculation. The density of the shading indicates the concentration of electrons formed in the avalanche. (From Matoba et al.[?])

Space charge limits the count rate!
(空間電荷)

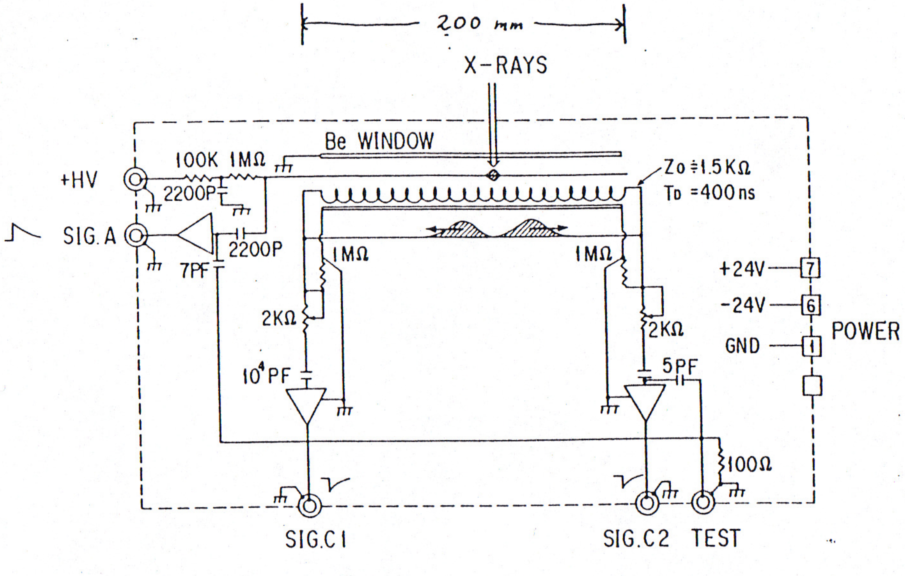

Schematic diagram of electronics of the linear PSD

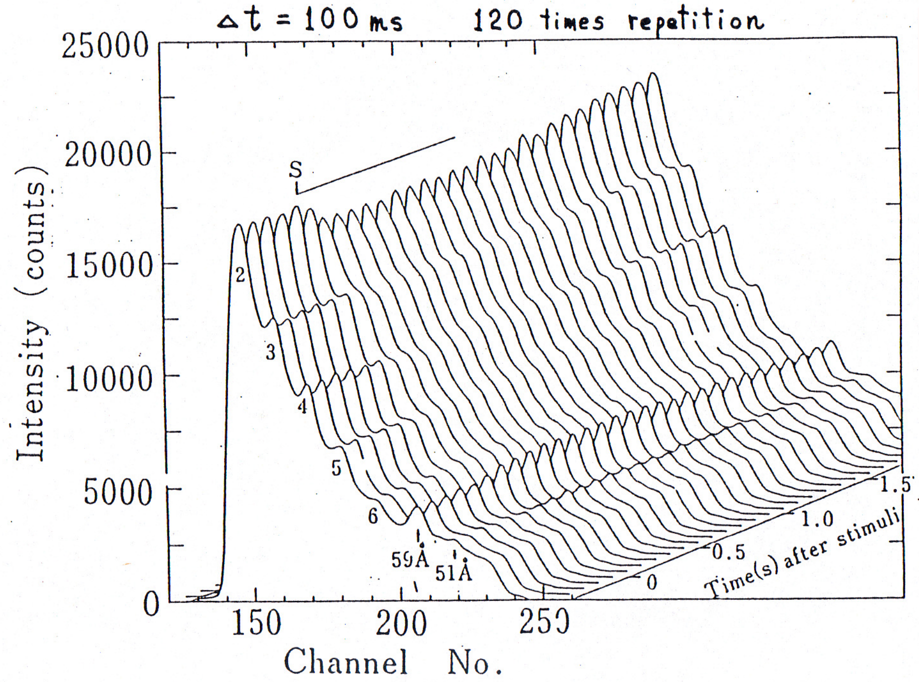

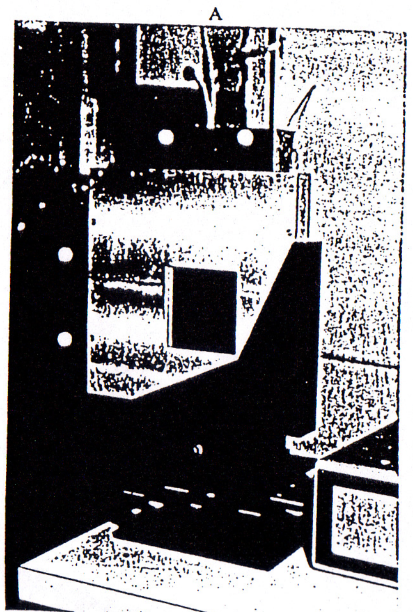

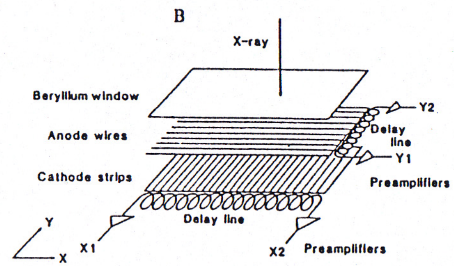

Fig. 1 Structure of the multi-wire chamber.
A: Front view of the two-dimensional detector.
B: The chamber consisted of a beryllium window, an anode and a cathode planes with a spacing 5 mm. The anode plane was made of gold-plated tungsten wires 10 μm in diameter, 2 mm apart, while cathode plane was made of the copper strips, 2 mm apart, orthogonal to the anode wires. The chamber was filled with a gas mixture of 90% argon and 10% methane at a pressure of 1 atm.

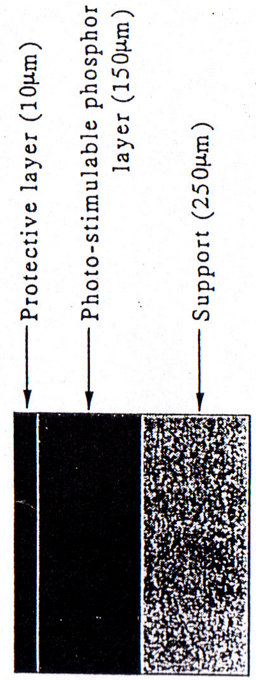

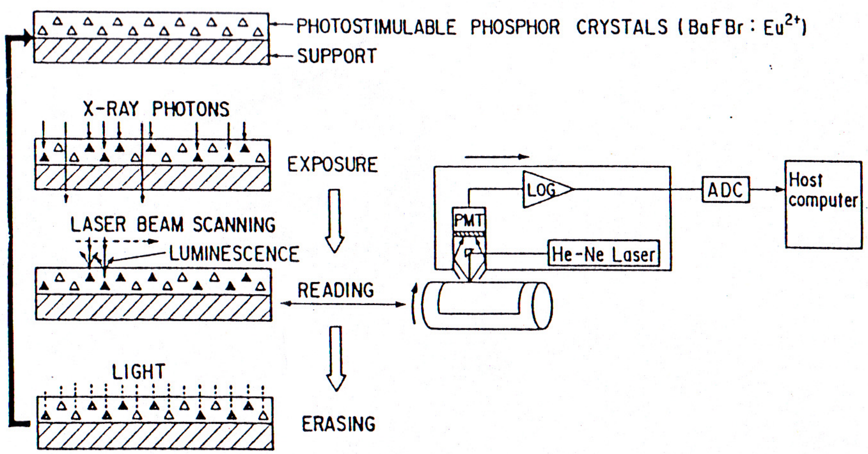

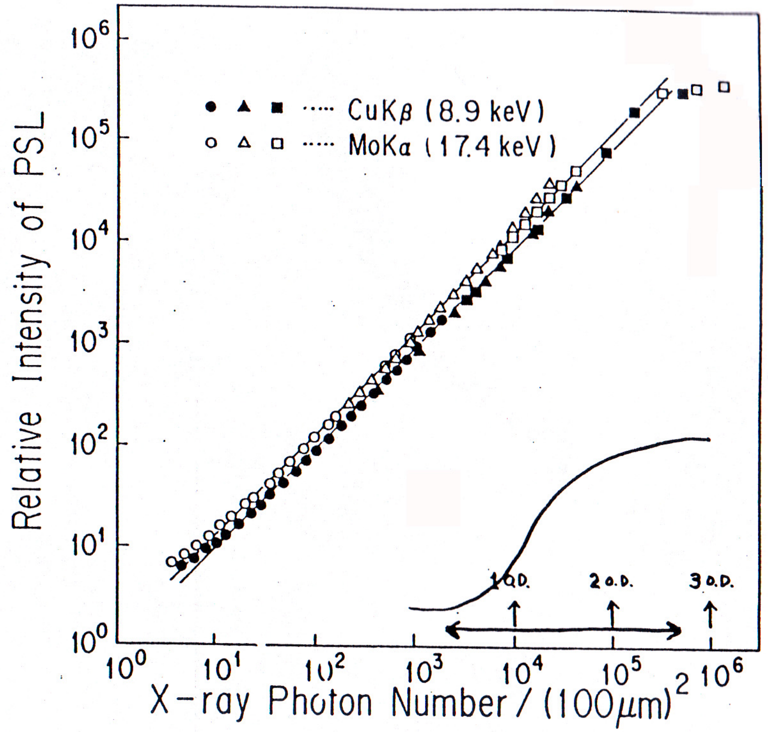

Photo-stimulated Luminescence Mechanisms

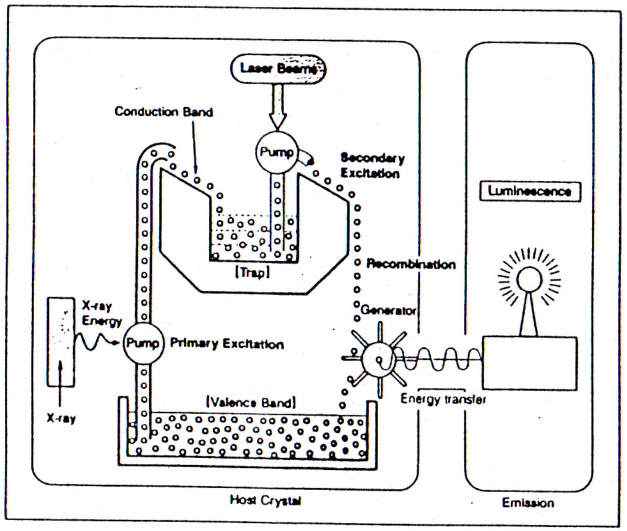

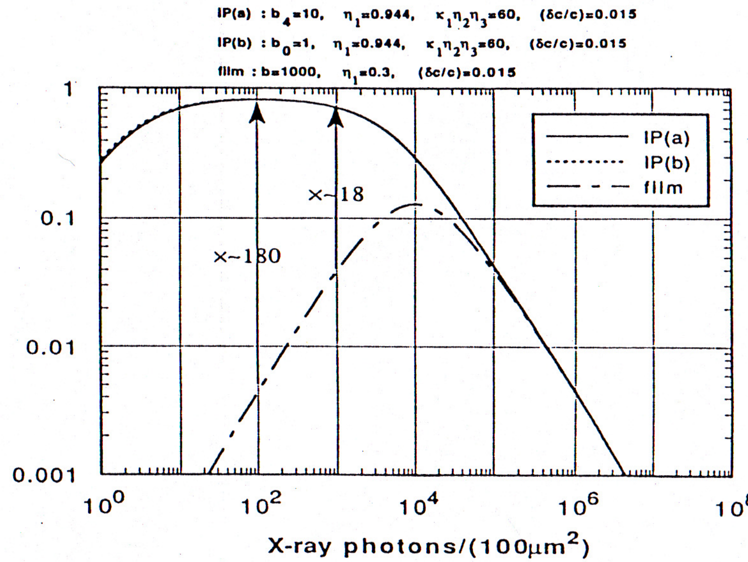

検出量子効率（DQE）の入射X線量依存性

[redacted]

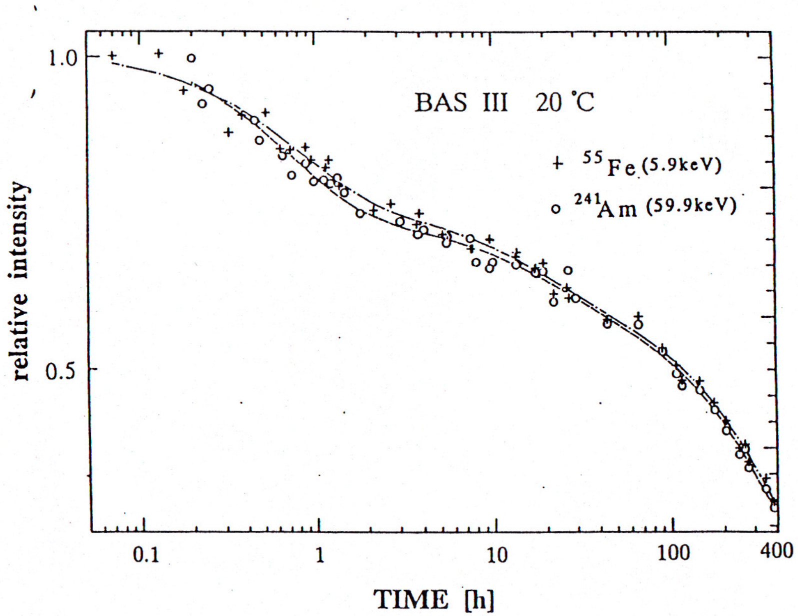

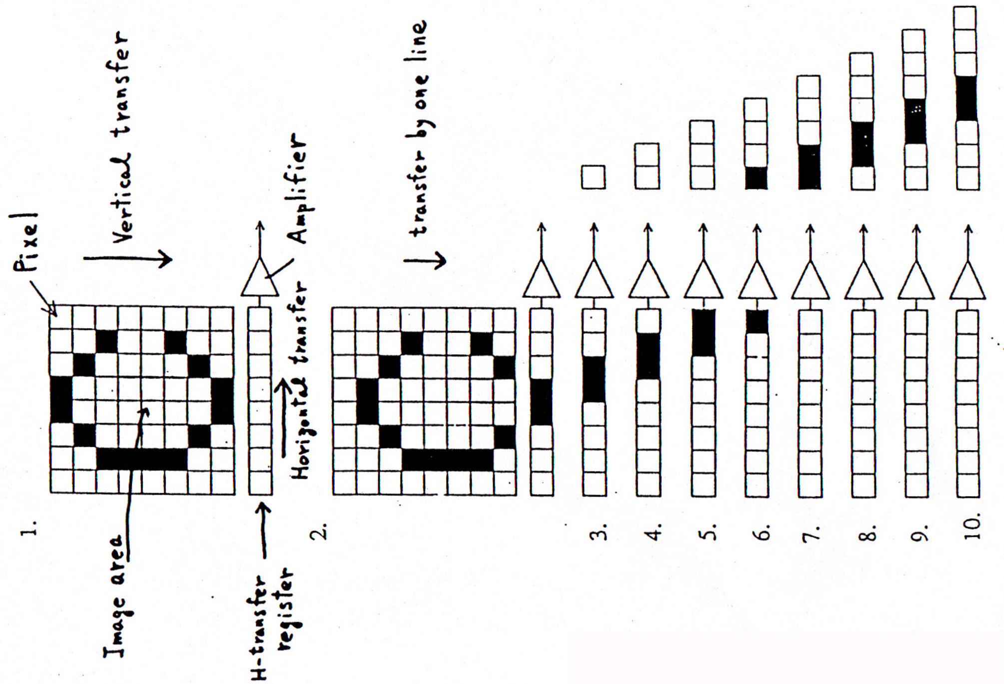

Application field of the Imaging Plates

Protein crystallography
- Weissenberg camera
- Oscillation camera
- Laue method

Laue diffraction of micro-crystal

Small-angle x-ray scattering

X-ray diffraction under high pressure

X-ray diffuse scattering

Compton X-ray scattering spectroscopy

Dispersive XAFS

X-ray topography

Angiography

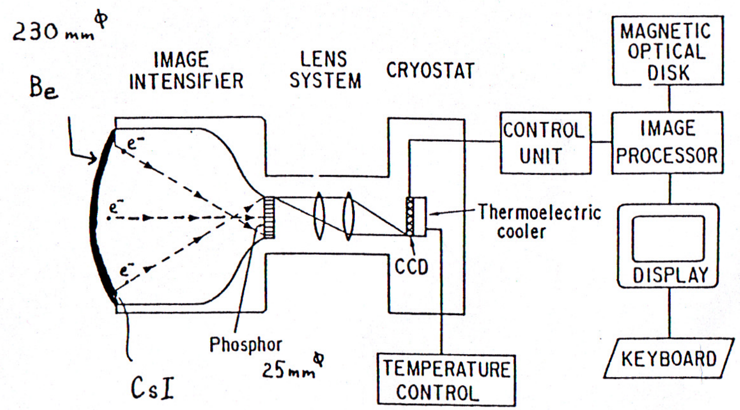

Schematics of the X-ray TV detector which utilizes the Be-window X ray image intensifier together with a cooled or a TV-rate CCD.

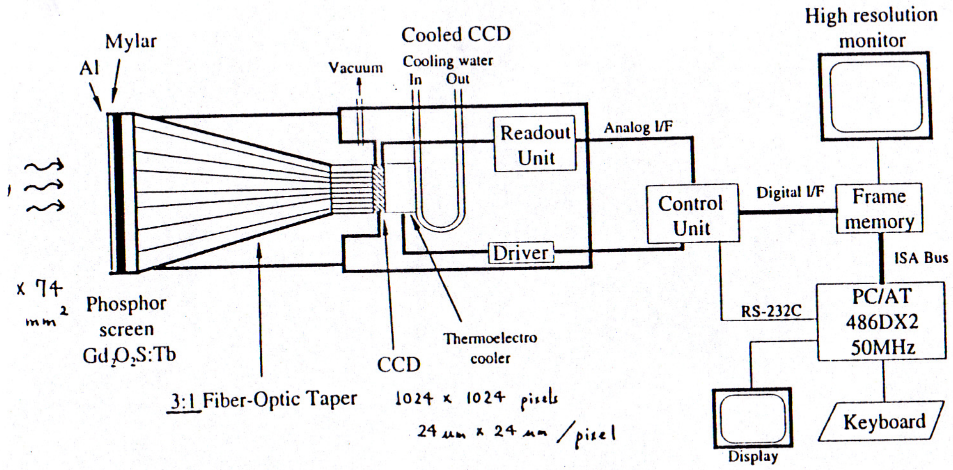

Schematics of a Fiber-coupled CCD detector

	Signal/xph / r.m.s. noise
IP	1 ~ 3
XII ⊕ CCD	5 ~ 10
FOT ⊕ CCD	0.3 ~ 1

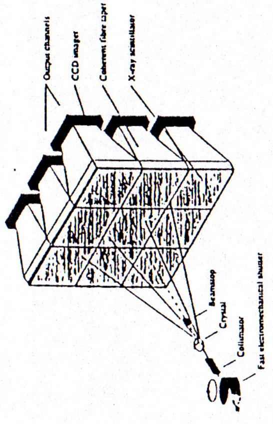

Figure 4
Example of a typical 3 × 3 mosaic CCD detector. The full active aperature of this system is approximately 150 × 150 mm. All the CCDs can be read out in parallel, with typically four output channels per device. Adapted from Westbrook (1988).

Comparison of three x-ray area detectors

	Advantage	Application	Drawback
IP	Good uniformity Large area size	static precise measurement slow time-resolved measurement	Long readout time 1~2 min. off-line
II+CCD	High DQE Short readout time 1~4 s	time-resolved measurement	Image distortion of II (variant) delicate, complex
FOT+CCD	Stability Short readout time 1~4 s	automated static measurement ↓ protein crystallography	Limited area size Image distortion of FOT (invariant)

CCD with multi-channel readout

CCDの多チャンネル読み出し

8チャンネル ⟶ 1000 frame/s (1 ms)

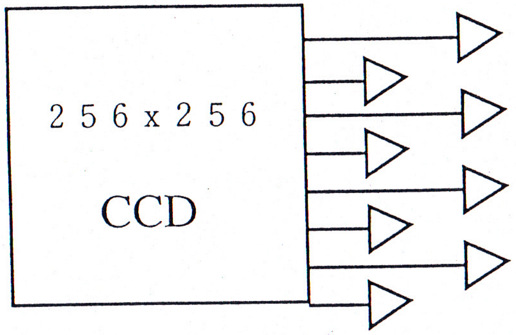

4x4 スーパーピクセル読み出し ⟶ 8000 frames/s (125 μs)
super-pixel readout

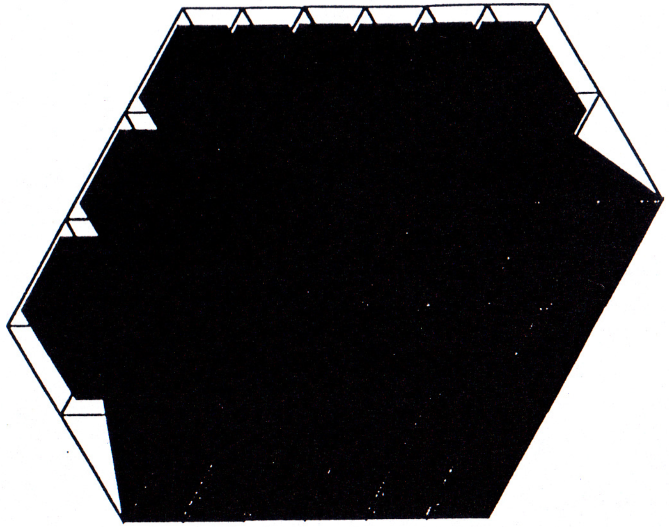

Schematics of the arrayed CCD x-ray detector (in the case of 3 × 6 system).

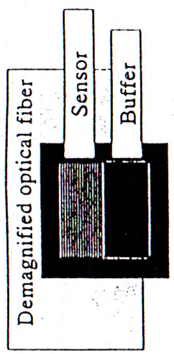

Coupled with demagnified optical fiber

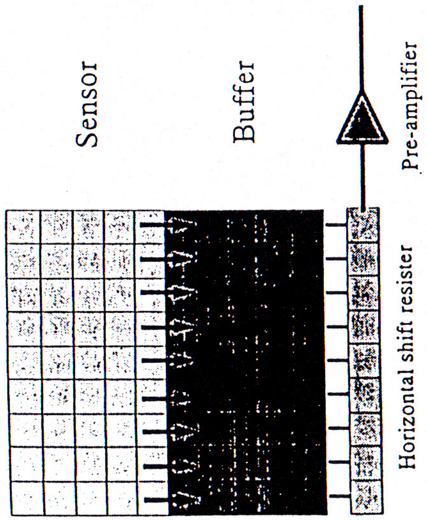

Buffered frame transfer-type CCD

PAD

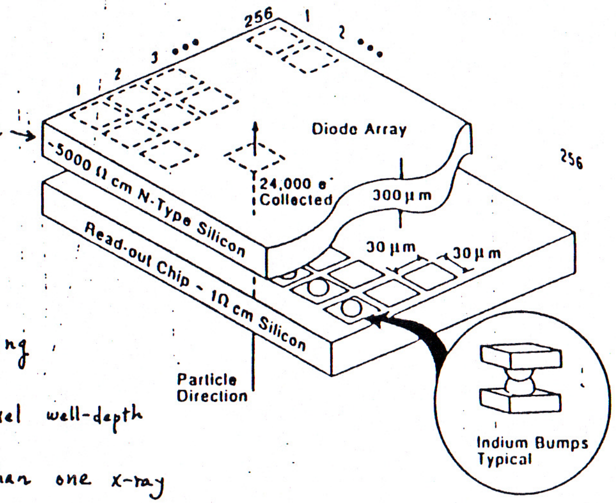

- 5 μs framing
- 10,000 xph/pixel well-depth
- noise less than one x-ray

PAD : Pixel Arrayed Detector

Basic Configuration

Separate Sensor + Readout Chips

Joined by 2-Dimensional Array

of Indium Bump Bonds

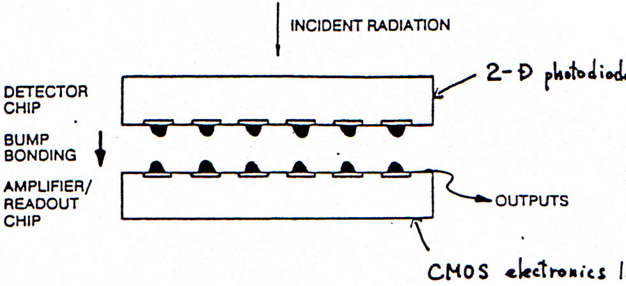

pixel : 150 μm x 150 μm

No. of pixel : 1024 x 1024